ELectronics EXpress

REVIEW PAPER

IEICE Electronics Express, Vol.13, No.18, 1–13

Recent progress in compound semiconductor electron devices

Yasuyuki Miyamoto[a)]

Department of Electrical and Electronic Engineering, Tokyo Institute of Technology, 2–12–1 Ookayama, Meguro-ku, Tokyo 152–8552, Japan

a) *miya@ee.e.titech.ac.jp*

Abstract: Compound semiconductor electronic devices have the capability to provide high-speed operation as they have higher mobility than Si. At present, compound semiconductor devices are popular as parts of consumer electronics such as wireless communication devices or satellite television. Introduction of wide bandgap compound semiconductors has increased the use of compound semiconductor devices in base stations of cellular phone systems and as replacements for vacuum tubes. More recently, the research on InGaAs MOSFET has been directed towards realization of its potential as an alternative for silicon.

This review explains the present commercialization of compound semiconductor devices in consumer electronics, and its state-of-art results such as the 529-GHz dynamic frequency divider using InGaAs heterojunction bipolar transistors, the 1-THz amplification provided by the InGaAs high–electron-mobility transistor (HEMT), and the power of 3 Wmm^{-1} provided by the GaN HEMT at 96 GHz. The InGaAs MOSFET as the next candidate for logic circuit components, is also explained.

Keywords: compound semiconductor, HBT, HEMT, MOSFET

Classification: Electron devices, circuits and modules

References

[1] N. Hirose and M. Fukuda, "Numerical Wind Tunnel (NWT) and CFD research at National Aerospace Laboratory," HPC Asia '97 (DOI: 10.1109/HPC.1997.592130).

[2] T. Mimura: "Development of high electron mobility transistor," Jpn. J. Appl. Phys. **44** (2005) 8263 (DOI: 10.1143/JJAP.44.8263).

[3] M. Fresina: "Trends in GaAs HBTs for wireless and RF," BTCM (2011) 150 (DOI: 10.1109/BCTM.2011.6082769).

[4] H. Kroemer: "Heterostructure bipolar transistors and integrated circuits," Proc. IEEE **70** (1982) 13 (DOI: 10.1109/PROC.1982.12226).

[5] Y. Kusakari, *et al.*: "Development of high efficiency RF power MOSFET for GSM cellular phone system," Trans. IEICE **E85-C** (2002) 1436.

[6] J. Young: "Mobile phone RF front end integrated roadmap," Semiconchina (2015).

[7] W. Snodgrass, *et al.*: "Pseudomorphic InP/InGaAs heterojunction bipolar transistors (PHBTs) experimentally demonstrating $f_T = 765$ GHz at 25°C increasing to $f_T = 845$ GHz at −55°C," IEDM (2006) (DOI: 10.1109/IEDM.

DOI: 10.1587/elex.13.20162002
Received July 22, 2016
Accepted August 5, 2016
Published September 25, 2016

2006.346853).
[8] T. Oka, *et al.*: "Small-scale InGaP/GaAs heterojunction bipolar transistors for high-speed and low-power integrated-circuit applications," Int. J. High Speed Electron. Syst. **11** (2001) 115 (DOI: 10.1142/S0129156401000800).
[9] U. Bhattacharya, *et al.*: "Transferred substrate Schottky-collector heterojunction bipolar transistors: first results and scaling laws for high f_{max}," Electron. Device Lett. **16** (1995) 357 (DOI: 10.1109/55.400737).
[10] V. Radisic, *et al.*: "InP HBT transferred substrate amplifiers operating to 600 GHz," MTT-S IMS (2015) (DOI: 10.1109/MWSYM.2015.7166750).
[11] K. Kurishima, *et al.*: "InP/InGaAs double-heterojunction bipolar transistor with step-graded InGaAsP collector," Electron. Lett. **29** (1993) 258 (DOI: 10.1049/el:19930177).
[12] M. Dahlstrom, *et al.*: "Wideband DHBTs using a graded carbon-doped InGaAs base," Electron. Device Lett. **24** (2003) 433 (DOI: 10.1109/LED.2003.815009).
[13] M. W. Dvorak, *et al.*: "300 GHz InP/GaAsSb/InP double HBTs with high current capability and $BV_{CEO} > 6$ V," Electron. Device Lett. **22** (2001) 361 (DOI: 10.1109/55.936343).
[14] B. Razavi: *Design of Integrated Circuits for Optical Communications* (McGraw-Hill, NY, 2003) 344.
[15] P. K. Tien: "Propagationdelay in high speed silicon bipolar and GaAs HBT digital circuits," Int. J. High Speed Electron. Syst. **1** (1990) 101 (DOI: 10.1142/S012915649000006X).
[16] M. Seo, *et al.*: "A 529 GHz dynamic frequency divider in 130 nm HBT process," IEICE Electron. Express **12** (2015) 20141118 (DOI: 10.1587/elex.12.20141118).
[17] J. Hacker, *et al.*: "InP HBT amplifier MMICs operating at 0.67 THz," MTT-S IMS (2013) (DOI: 10.1109/MWSYM.2013.6697518).
[18] M. Rodwell, *et al.*: "THz Indium Phosphide bipolar transistor technology," CSICS (2012) (DOI: 10.1109/CSICS.2012.6340091).
[19] A. Baraskar, *et al.*: "High doping effects on in-situ ohmic contacts to n-InAs," IPRM (2010) 1 (DOI: 10.1109/ICIPRM.2010.5516269).
[20] K. Tanaka, *et al.*: "InP HBT with 55-nm-wide emitter and relationship between emitter width and current density," IPRM (2012) 188 (DOI: 10.1109/ICIPRM.2012.6403354).
[21] W. Liu: *Fundamentals of III-V Devices* (John Wiley and Sons, 1999) 471.
[22] L. McCarthy, *et al.*: "GaN HBT: Toward an RF device," Trans Electron. Dev. **48** (2001) 543 (DOI: 10.1109/16.906449).
[23] T. Makimoto, *et al.*: "High current gains obtained by InGaN/GaN double heterojunction bipolar transistors with p-InGaN base," Appl. Phys. Lett. **79** (2001) 380 (DOI: 10.1063/1.1387261).
[24] C. Mazure and G. Cesana: "SOI based platform for IoT optimized applications," Semiconchina (2016).
[25] B.-S. Hong, *et al.*: "Novel Bi-HEMT technology for LTE handset application," CS Mantech (2012).
[26] X. Mei, *et al.*: "First demonstration of amplification at 1 THz Using 25-nm InP high electron mobility transistor process," Electron. Dev. Lett. **36** (2015) 327 (DOI: 10.1109/LED.2015.2407193).
[27] T.-W. Kim, *et al.*: "Logic characteristics of 40 nm thin-channel InAs HEMTs," IPRM (2010) (DOI: 10.1109/ICIPRM.2010.5516257).
[28] E.-Y. Chang, *et al.*: "InAs thin-channel high-electron-mobility transistors with very high current-gain cutoff frequency for emerging submillimeter-wave applications," Appl. Phys. Express **6** (2013) 034001 (DOI: 10.7567/APEX.6.034001).

DOI: 10.1587/elex.13.20162002
Received July 22, 2016
Accepted August 5, 2016
Published September 25, 2016

[29] A. Tessmann, *et al.*: "Submillimeter-wave amplifier circuits based on thin film microstrip line front-side technology," CSICS (2015) (DOI: 10.1109/CSICS.2015.7314526).
[30] A. Hirata, *et al.*: "10-Gbit/s wireless link using InP HEMT MMICs for generating 120-GHz-band millimeter-wave signal," Trans. MTT **57** (2009) 1102 (DOI: 10.1109/TMTT.2009.2017256).
[31] H.-J. Song and T. Nagatsuma: "Present and future of terahertz communications," IEEE Trans. Terahertz Sci. Technol. **1** (2011) 256 (DOI: 10.1109/TTHZ.2011.2159552).
[32] O. Ambacher, *et al.*: "Role of spontaneous and piezoelectric polarization induced effects in group-III nitride based heterostructures and devices," Phys. Stat. Solidi (b) **216** (1999) 381 (DOI: 10.1002/(SICI)1521-3951(199911)216:1<381::AID-PSSB381>3.0.CO;2-O).
[33] U. Mishra, *et al.*: "GaN-based RF power devices and amplifiers," Proc. IEEE **96** (2007) 287 (DOI: 10.1109/JPROC.2007.911060).
[34] D. Schmelzer, *et al.*: "A GaN HEMT class F amplifier at 2 GHz with >80% PAE," J. Solid-State Circuits **42** (2007) 2130 (DOI: 10.1109/JSSC.2007.904317).
[35] A. Kawano, *et al.*: "High-efficiency and wide-band single-ended 200 W GaN HEMT power amplifier for 2.1 GHz W-CDMA base station application," APMC (2005) (DOI: 10.1109/APMC.2005.1606618).
[36] H. Shigematsu, *et al.*: "C-band 340-W and X-band 100-W GaN power amplifiers with over 50-% PAE," MTT-S IMS (2009) (DOI: 10.1109/MWSYM.2009.5165934).
[37] K. Shinohara, *et al.*: "Scaling of GaN HEMTs and Schottky diodes for submillimeter-wave MMIC applications," Trans. Electron.Devices **60** (2013) 2982 (DOI: 10.1109/TED.2013.2268160).
[38] K. Makiyama, *et al.*: "Collapse-free high power InAlGaN/GaN-HEMT with 3 W/mm at 96 GHz," IEDM (2015) (DOI: 10.1109/IEDM.2015.7409659).
[39] W. Saito, *et al.*: "Recessed-gate structure approach toward normally off high-voltage AlGaN/GaN HEMT for power electronics," IEEE Trans. Electron Devices **53** (2006) 356 (DOI: 10.1109/TED.2005.862708).
[40] Y. Cai, *et al.*: "High-performance enhancement-mode AlGaN/GaN HEMTs using fluoride-based plasma treatment," Electron. Device Lett. **26** (2005) 435 (DOI: 10.1109/LED.2005.851122).
[41] Y. Uemoto, *et al.*: "Gate injection transistor (GIT)-A normally-off AlGaN/GaN power transistor using conductivity modulation," Trans. Electron. Devices **54** (2007) 3393 (DOI: 10.1109/TED.2007.908601).
[42] S. Chowdhury and U. K. Mishra: "Lateral and vertical transistors using the AlGaN/GaN heterostructure," Trans. Electron. Devices **60** (2013) 3060 (DOI: 10.1109/TED.2013.2277893).
[43] N. Kaminski, *et al.*: "SiC and GaN devices - Competition or coexistence?" CIPS (2012).
[44] P. D. Ye, *et al.*: "GaAs metal-oxide-semiconductor field-effect transistor with nanometer-thin dielectric grown by atomic layer deposition," Appl. Phys. Lett. **83** (2003) 180 (DOI: 10.1063/1.1590743).
[45] V. Chobpattana, *et al.*: "Scaled ZrO_2 dielectrics for $In_{0.53}Ga_{0.47}As$ gate stacks with low interface trap densities," Appl. Phys. Lett. **104** (2014) 182912 (DOI: 10.1063/1.4875977).
[46] A. G. Lind, *et al.*: "Comparison of thermal annealing effects on electrical activation of MBE grown and ion implant Si-doped $In_{0.53}Ga_{0.47}As$," J. Vac. Sci. Technol. B **33** (2015) 021206 (DOI: 10.1116/1.4914319).
[47] E. Tokumitsu: "Correlation between Fermi level stabilization positions and maximum free carrier concentrations in III-V compound semiconductors," Jpn.

DOI: 10.1587/elex.13.20162002
Received July 22, 2016
Accepted August 5, 2016
Published September 25, 2016

J. Appl. Phys. **29** (1990) L698 (DOI: 10.1143/JJAP.29.L698).
[48] M. Egard, *et al.*: "High transconductance self-aligned gate-last surface channel $In_{0.53}Ga_{0.47}As$ MOSFET," IEDM (2011) (DOI: 10.1109/IEDM.2011.6131544).
[49] Y. Yonai, *et al.*: "High drain current (>2 A/mm) InGaAs channel MOSFET at $V_D = 0.5$ V with shrinkage of channel length by InP anisotropic etching," IEDM (2011) (DOI: 10.1109/IEDM.2011.6131545).
[50] S. Takagi, *et al.*: "Carrier-transport-enhanced channel CMOS for improved power consumption and performance," IEEE Trans. Electron Devices **55** (2008) 21 (DOI: 10.1109/TED.2007.911034).
[51] L. Czornomaz, *et al.*: "Co-integrating high mobility channels for future CMOS, from substrate to circuits," IPRM (2014) (DOI: 10.1109/ICIPRM.2014.6880563).
[52] N. Waldron, *et al.*: "InGaAs gate-all-around nanowire devices on 300 mm Si substrates," Electron. Device Lett. **35** (2014) 1097 (DOI: 10.1109/LED.2014.2359579).
[53] K. Ohsawa, *et al.*: "Channel thickness dependence on InGaAs MOSFET with n-InP source for high current density," IEICE Electron. Express **11** (2014) 20140567 (DOI: 10.1587/elex.11.20140567).
[54] C.-Y. Huang, *et al.*: "12 nm-gate-length ultrathin-body InGaAs/InAs MOSFETs with 8.3×10^5 I_{ON}/I_{OFF}," DRC (2015) (DOI: 10.1109/DRC.2015.7175669).
[55] A. Vardi and J. A. del Alamo: "Sub-10 nm fin-width self-aligned InGaAs FinFETs," Electron. Dev. Lett. **37** (2016) 1104 (DOI: 10.1109/LED.2016.2596764).
[56] Y. Mishima, *et al.*: "InGaAs tri-gate MOSFETs with MOVPE regrown source/drain," DRC (2014) (DOI: 10.1109/DRC.2014.6872327).
[57] E. Memisevic, *et al.*: "Scaling of vertical InAs/GaSb nanowire tunneling field-effect transistors on Si," Electron. Device Lett. **37** (2016) 549 (DOI: 10.1109/LED.2016.2545861).

1 Introduction

Compound semiconductors exhibit superior characteristics when used as materials for electronic devices, compared to Si. For example, the electron mobility is higher than that of Si; furthermore, the semi-insulating substrate provides a low leakage current and small parasitic capacitance, resulting in higher speed of operation. The transition from Si to compound semiconductors has been predicted for over 50 years. In 1993, Fujitsu developed the most powerful computer in the world, a supercomputer based on the GaAs MESFET [1]. However, the progress in the miniaturization of CMOS circuits has reduced the power consumption, processing time and prices continuously. At present, almost all the logic circuits, including supercomputers, are composed of Si CMOS circuits.

On the other hand, the merits of the high speeds provided by compound semiconductors were demonstrated in wireless applications at high frequencies. The starting point in consumer applications was the low-noise preamplifier using a high–electron-mobility transistor (HEMT) for satellite broadcasting in the 10-GHz band, introduced in 1987 [2]. The next big market was that of the GaAs hetero-junction bipolar transistor (HBT) used as a power amplifier for cellular phones in the late 90s [3].

DOI: 10.1587/elex.13.20162002
Received July 22, 2016
Accepted August 5, 2016
Published September 25, 2016

In this paper, the recent progress of HBTs and HEMTs, which are the commonly used transistors in consumer electronics, are explained after a brief introduction of each device. Applications of materials such as, GaAs, InGaAs and GaN in HEMT and HBT are discussed. Then, the InGaAs MOSFETas the next candidate for logic devices is explained.

2 HBT

HBT was proposed to prevent hole injection from the base to the emitter by using a wide bandgap emitter [4] because the current gain in conventional Si bipolar transistors are limited by the hole injection. When the composition change at emitter–base junction is gradual, the bandgap difference prevents the hole injection. In the usual case of an abrupt composition change in the emitter–base junction, the band discontinuity of the valence band prevents the hole injection. Even when there exists a band discontinuity for the valence band, suppression of hole injection is usually enough. Thus, the base can be heavily doped, without causing a large amount of hole injection in the HBT, which results in a lower base resistance. When the hole injection is suppressed in the HBT, recombination such as the Auger recombination caused by the heavy doping in the base decides the base current.

As described before, the most popular HBT is the GaAs HBT used in the power amplifier of cellular phones. Usually, InGaP is chosen as the wide bandgap emitter and the GaAs base layer is heavily doped with C. The lightly doped drain (LDD) MOSFET derived from the Si MOSFET became popular as the power amplifier in cellular phones because of its low price [5] for a while. Recently, Si-MOS power amplifiers based on the silicon-on-insulator (SOI) structure are also in the market. However, HBT continues to dominate the main stream of power amplifiers of cellular phones, due to its high efficiency, as well as high linearity required for improved frequency utilization efficiency [6].

At present, the InGaAs HBT lattice-matched to InP substrate has the highest cutoff frequency (f_T) among all transistors. Fig. 1 shows the schematic structure of an InGaAs HBT. By using a heavily doped base, the thickness of the base layer is reduced. The base transit time, which is the most significant component in Si bipolar transistors, can be reduced by using a higher electron diffusion constant in the base layer.

For high-speed operation of the HBT, thickness reduction of the electron-propagating base/collector layers is required for reducing the transit time, and a high emitter-current density is required for reducing the charging time. At present, the highest f_T is 765 GHz [7]. The epitaxial structure has a 12.5-nm-thick base and a 55-nm-thick collector. The current density is 1.87 $MAcm^{-2}$. However, a high current density without reduction of the emitter width causes high power consumption that raises the temperature into the prohibited range. Thus, reduction of the emitter width by electron beam lithography is necessary. The scanning electron microscope (SEM) image of the mesa structure fabricated using electron beam lithography is shown as a part of Fig. 1. The emitter width is 100 nm. When the emitter is narrow, a proportional narrowing of the collector is ideal for a high maximum oscillation frequency (f_{max}). As the collector capacitance under the base

DOI: 10.1587/elex.13.20162002
Received July 22, 2016
Accepted August 5, 2016
Published September 25, 2016

electrode is a parasitic capacitance, the width of the base electrode must be the minimum [8]. In case of Fig. 1, the total base mesa width is 400 nm. Because of a low base contact resistance, taking the base width and separation between emitter mesa and base electrode into account, it is difficult to obtain a completely proportional width for the base mesa using conventional methods; the ratio changes according to the requirements of the application [8]. To obtain the collector width identical to emitter width, the transferred-substrate method was proposed [9]. In this method, after formation of emitter and base, the substrate is bonded to the other substrate upside down, and a collector electrode aligned with the emitter electrode is fabricated on the opposite side of the base epitaxial layer after removing the mother substrate. The transferred-substrate method also has the possibility to overcome the limitation of low thermal conductivity in the InP substrate [10].

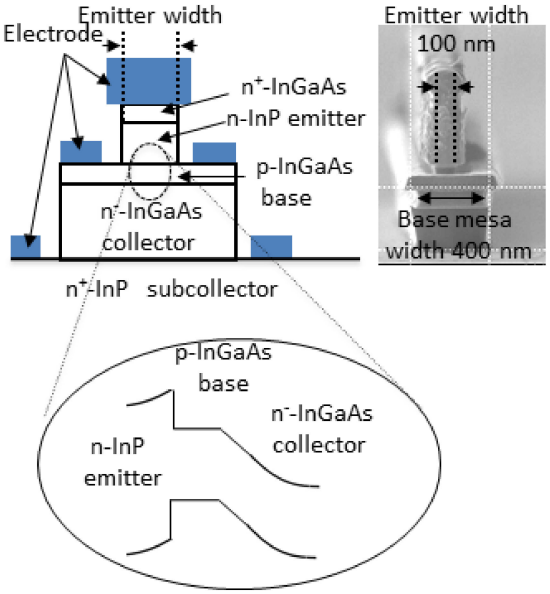

Fig. 1. Schematic cross-section of InP HBT, and SEM view of fabricated HBT mesa structure. The inset shows the band structure of the HBT.

When the base and collector materials are the same, smooth electron injection is obtained. However, to obtain a high breakdown voltage, introduction of a double heterojunction bipolar transistor (DHBT) is required. In a DHBT, although a wide bandgap collector provides a high breakdown voltage, smooth current injection from the base to the collector is prevented by the conduction-band discontinuity. Insertion of quaternary [11] or superlattice [12] layers between the base and collector is effective to obtain a smooth current flow. When GaAsSb is used as a base, the heterojunction with InP becomes a Type II or staggered junction, and smooth electron injection is obtained although the diffusion constant of GaAsSb is lower than that of InGaAs [13].

In case of FETs, the threshold voltage may be changed by gate size by short channel effect. However, in case of HBT, change of size of emitter or base is not related to the threshold voltage [4]. This characteristics is suitable for apply the

DOI: 10.1587/elex.13.20162002
Received July 22, 2016
Accepted August 5, 2016
Published September 25, 2016

HBTs to high-speed logic circuits. The present logic circuits based on bipolar transistors use either emitter-coupled logic or current-mode logic (CML), and their power consumption is higher than that of complete CMOS circuits. However, the CML configuration is used for high-speed logic applications in CMOS circuits also [14]. Thus, it is not a significant drawback. As the operation speed of CML circuits can be estimated from f_T and f_{max} [15], the improvements in the RF applications are directly connected to the improvements in the digital circuits. A dynamic frequency divider operated at 529 GHz using a HBT with a 130-nm-wide emitter, f_T of 520 GHz, and f_{max} of 1.1 THz, was reported [16]. In analog applications, gains up to 20 dB and powers up to 0.86 mW at 670 GHz were reported [17]. The predicted HBT performance could be delivered based on the scheme of scaling [18]. If an emitter width of 64 nm, emitter contact resistance of $2 \times 10^{-8}\ \Omega\text{cm}^2$, and an emitter current density of $3.6\ \text{MAcm}^{-2}$ were obtained simultaneously, a performance with $f_T = 520$ GHz and $f_{max} = 1.1$ THz could be predicted. An n-type contact resistivity of $6 \times 10^{-9}\ \Omega\text{cm}^2$ [19] by the in-situ deposition of Mo after crystal growth, and a current density of $5\ \text{MAcm}^{-2}$ with a 55-nm-wide emitter [20], have already been reported. However, as the fabrication process for HBT is complicated as compared to that of HEMT [21], a combination of all the required conditions has not been realized until now.

GaN HBTs can obtain high breakdown voltages due to their wide bandgaps. A high breakdown voltage from a thin collector can provide high speed, high efficiency, and high power, simultaneously. However, the formation of a p-type base layer is difficult because of the low activation efficiency of p-type doping. For example, as the activation efficiency is around 1.5% in GaN, a doping concentration of approximately $10^{19}\ \text{cm}^{-3}$ results in a carrier concentration of approximately $10^{17}\ \text{cm}^{-3}$ [22]. By using InGaN, the efficiency can be improved. However, the efficiency is still around 50% only [23]. Moreover, as the diffusion constant of Mg (typical p-type dopant for GaN) is too large when compared to that of C (typical p-type dopant for GaAs HBTs or InGaAs HBTs), the shift in the electrical junction because of the diffusion of dopants must be taken into account. Because of these problems, reports of GaN HBTs have reduced recently.

3 HEMT

In HEMT, the two-dimensional electron gas (2DEG) formed by the modulation-doped heterostructure has a high mobility. The electron speed reaches its peak velocity rapidly because of the high electron mobility. The combination of high electron mobility and high electron concentration reduces the low sheet resistance, resulting in a low contact resistance. 2DEG also provides suppression of short-channel effects by the confinement of the vertical electron distributions in the channel. The heterostructure of GaAs HEMTs was derived from a combination of an n-doped AlGaAs layer as the electron-supply layer and an undoped GaAs channel. Recently, a combination of AlGaAs and InGaAs layers is also becoming popular for obtaining higher electron mobility. A GaAs HEMT with an InGaAs channel is called a pseudomorphic HEMT because the lattice of the channel has a strain from a different lattice constant (of the GaAs substrate). Often pseudomor-

DOI: 10.1587/elex.13.20162002
Received July 22, 2016
Accepted August 5, 2016
Published September 25, 2016

phic HEMTs are called pHEMTs for short. It is to be noted that the carriers in pHEMT are electrons.

Commercialization of the GaAs HEMT started from the low-noise preamplifiers for radio telescopes [2]. However, the production level was small. Then, as part of consumer electronics, HEMTs became popular as low-noise preamplifiers for satellite broadcasting. The commercialization was based on the low-noise feature of HEMTs. To my knowledge, all antennas for satellite broadcasting use HEMTs as the preamplifiers.

The main function of GaAs HEMTs in cellular phones is antenna switching. However, SOI antenna switches have become quite popular due to the recent progress made in RF-SOIs [24]. It is to be noted that the advantages of GaAs are in their use in power amplifiers. Thus, the Bi-HEMT, which is an integrated circuit of HBT and HEMT using a stacked epitaxial structure [25], can provide an attractive integration of the power amplifier with the antenna switch, and the application area can be expanded to Wi-Fi.

At present, amplification at the highest frequency of the transistor is carried out by InGaAs HEMT lattice-matched to InP substrate [26]. The delays in the intrinsic parts of the HEMT can be calculated by dividing the channel length by the electron speed. Thus, shortening the channel and improving the electron speed are required for high-speed operation.

The schematic structure of the InGaAs HEMT is shown in Fig. 2. The shortening of the channel is achieved by reducing the gate-electrode length. When the gate length is shorter than 100 nm, a T-gate structure is popularly used to prevent the increase in gate resistance that results in a degradation of f_{max}. The T-gate structure is fabricated using a 3-layer resist as shown in the SEM picture in Fig. 2 and metal evaporation. Please note that simple gate reduction, without reduction in the vertical scale, introduces short-channel effects, i.e., degradation of the controllability of the current by the gate. To reduce the distance from the channel to the gate, thickness reduction of the upper AlInAs epitaxial layer and slight etching of the underside of the gate just before formation of the gate metal, are effective. Reduction of channel thickness is also effective, although mobility degradation is introduced because of the thin channel [27].

To increase the electron velocity in the channel, acceleration of the electron when the electron enters the channel is important, and high electron mobility is effective for the acceleration. Thus, a higher In composition in the channel must be used for obtaining a higher mobility. For example, we used a composite channel consisting of a 2-nm-thick InAs channel sandwiched between a 2-nm-thick $In_{0.7}Ga_{0.3}As$ lower channel and a 1-nm-thick $In_{0.7}Ga_{0.3}As$ upper channel, as shown in the inset of Fig. 2 [28]. The electrons were supplied from the δ-doping in the upper InAlAs layer, and the observed mobility was 11,000 $cm^2V^{-1}s^{-1}$. To reduce the sheet resistance, the sheet carrier concentration of 2DEG was set as 3×10^{12} cm^{-2} and the obtained f_T was over 700 GHz.

δ-doping was performed in the lower layers of devices to increase the sheet carrier density. It is also useful in obtaining amplification at the highest frequency [26]. The observed sheet carrier density was 4×10^{12} cm^{-2} and the transconductance was over 3 S/mm, even when the contact resistance was included. The gate

DOI: 10.1587/elex.13.20162002
Received July 22, 2016
Accepted August 5, 2016
Published September 25, 2016

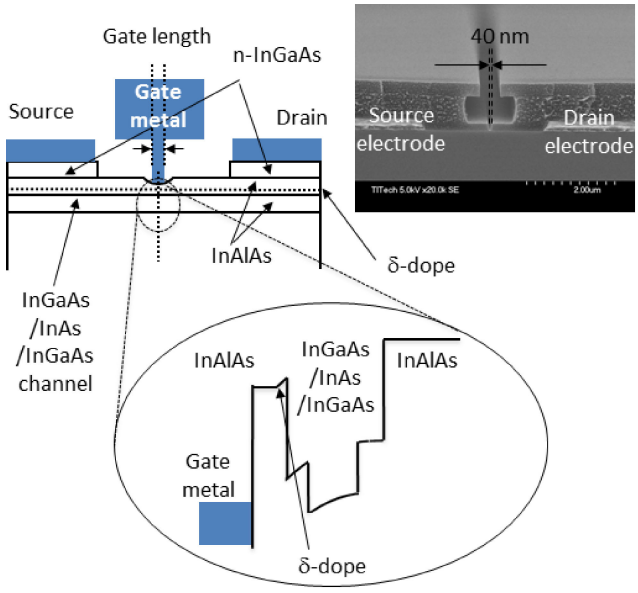

Fig. 2. Schematic cross-section of InGaAs HEMT and SEM view of 3-layer resist system on HEMT wafers. The band structure around the channel is shown in the inset.

length was 25 nm and f_{max} was 1.5 THz. A common-source design for a 10-stage amplifier using this HEMT shows a 9-dB gain at 1.0 THz.

As the short-channel effects are significant when the gate length shrinks (as described before), the shortest gate length that can offer a good microwave performance is limited to 20 nm in HEMTs [29]. This device exhibits excellent performances, such as a transconductance of 2.85 S/mm, f_T of 660 GHz, and f_{max} over 1 THz. Moreover, this device was fabricated on a GaAs substrate as a metamorphic HEMT (MHEMT), i.e., the lattice constant around the channel was equal to that of InP even on a GaAs substrate. As the largest commercialized diameter for the InP substrate was limited to 100 mm, larger GaAs substrates (with up to 200-mm diameter) have advantages when integrated in monolithic microwave integrated circuits (MMICs).

The main area of InGaAs HEMT applications is the amplification of sub-millimeter waves for communication and imaging. For frequencies over 100 GHz, InGaAs HEMT is the most suitable device to realize practical gain and power. Higher frequencies can easily provide higher bit rates. For example, a transmission of 10 Gb was realized in the 120-GHz band [30]. In the Beijing Olympic Games in 2008, this system was utilized to relay HD video signals of live TV shows from a studio to the International Broadcast Center over a distance of approximately 1 km [31].

GaN HEMTs can obtain higher sheet carrier densities than other HEMTs because the generation of 2DEG is due to spontaneous and piezoelectric polarizations [32]. Conventional AlGaN/GaN HEMTs have a sheet carrier density of 1 to 2×10^{13} cm^{-2} [33]. This number is about 10 times larger than that of GaAs/AlGaAs or InGaAs/InAlAs systems. Their mobility is between 1,000 to 2,000 cm^{2}V^{-1}s^{-1}, which is one order lower than that of InGaAs. However, because of the high sheet carrier concentration, the sheet conductivity is almost equal to or higher

DOI: 10.1587/elex.13.20162002
Received July 22, 2016
Accepted August 5, 2016
Published September 25, 2016

than that of InGaAs. As the breakdown electric field of 3.3 $MVcm^{-1}$ is one order higher than that of GaAs, a high voltage can be applied over a short distance.

This high breakdown electric field is effective in realizing high efficiencies in microwave amplifiers because the simplest way to increase the efficiency is by using large signal-voltage amplitudes in devices with high breakdown voltages. For example, 82% efficiency and 16-W power could be realized simultaneously by using GaN HEMTs with drain voltages of 42 V in the 2-GHz band [34]. These superior characteristics were commercialized for use in power amplifiers of base stations in the 2.1-GHz band for W-CDMA cellular phones [35]. Moreover, the replacement of vacuum tubes with solid-state power amplifiers for high-power microwave applications such as satellite communication or radar systems was realized by using GaN HEMTs [36].

The highest speed of GaN HEMT was observed in a device with 20-nm gate length and an AlGaN back barrier to suppress short-channel effects [37] as shown in Fig. 3. The top barrier layer was of AlN, for strong confinement and high sheet carrier density. The thickness of the GaN channel sandwiched by the top barrier and the back barrier was 20 nm. The gate–channel distances from the AlN top barrier layer and the GaN cap layer were 6 nm (for normally ON operation) and 4.5 nm (for normally OFF operation). To reduce the contact resistance, GaN regrowth was also used. Microwave performances of the devices were $f_T > 400$ GHz and $f_{max} > 400$ GHz, simultaneously. As the threshold voltages of the devices could be changed from the normally OFF mode to the normally ON mode, by a slight dry etching of the GaN cap and regrowth, an E/D-mode DCFL ring oscillator could be fabricated. A 501-stage ring oscillator exhibited 7.5 ps/stage.

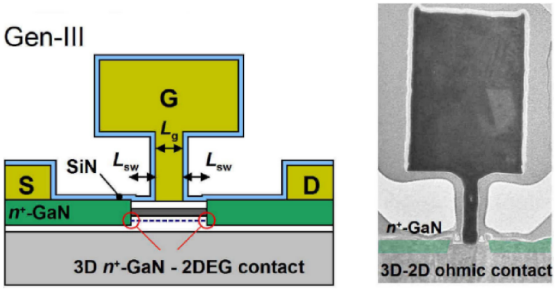

Fig. 3. Schematic cross-sectional view of 20-nm GaN HEMT, and transmission electron microscope image of T gate [37].

When the InAl(Ga)N system is introduced into the upper layer, the presence of large spontaneous charge can provide higher sheet carrier density of 2DEG without large lattice mismatch. At present, there are several issues with the crystal quality of the InAlN system which results in leaky devices. InAlGaN. InAlGaN is an attractive material for the barrier. By using the InAlGaN barrier, a power density of 3 Wmm^{-1} could be obtained in the 96-GHz band [38]. The drain bias was 20 V. The power was limited by the output power of the driver circuit and a power density of 3.6 Wmm^{-1} was obtained in the 86-GHz band.

Because of their high breakdown voltages, the GaN HEMTs have many promising applications in the power-electronics area. However, these power-elec-

DOI: 10.1587/elex.13.20162002
Received July 22, 2016
Accepted August 5, 2016
Published September 25, 2016

tronics applications require transistors in the normally-OFF mode while the conventional GaN HEMT operates under the normally-ON mode. Thus, threshold voltage shifts by using the etching of the surface [39], fluoride-based plasma treatments [40], or insertion of a p-layer into the gate [41], were reported. However, present commercialization of GaN HEMTs for power electronics starts from the cascade configuration [42] in which a normally-OFF low-voltage Si FET is connected to a normally-ON high-voltage GaN HEMT in series and the gate of GaN HEMT is connected to the source of Si FET. The present GaN HEMTs are mainly formed laterally, and the devices based on SiC (having wide bandgaps similar to GaN) are mainly formed with vertical structures suitable for several kV applications. Hence, the predicted voltage handled by GaN power devices are under 1 kV [43].

4 MOSFET

At present, almost all logic circuits are fabricated using Si-CMOS configurations. This is due to the low power dissipation in the static mode of CMOS. As other logic circuits involve high power dissipations in the static mode, they cannot beat the CMOS configuration. However, because one of the limitations of Si is its mobility, the III–V semiconductors have the potential to become the channel materials for n-MOSFETs. (Ge is the most promising channel material for p-MOSFET).

For logic applications of III–V MOSFETs, we faced three problems—interface state density, on current, and formation on Si substrate.

High interface state density at the semiconductor–insulator interface degraded the controllability of the gate. This poor controllability stopped the development of GaAs MOSFETs in the 90s. When atomic layer deposition became popular for the formation of high-k insulators, removal of the native oxides of the III–V materials by trimethylaluminum as a precursor to Al_2O_3 provided superior FET characteristics [44]. This report became a breakthrough for III–V MOSFETs. At present, by incorporating other surface treatments, interface state densities of approximately $10^{12}\,cm^{-2}eV^{-1}$ were reported at equivalent oxide thicknesses less than 1 nm [45]. These values are sufficient for a subthreshold slope steeper than $70\,mVdec^{-1}$.

As the motivation for using III–V MOSFETs is a high-mobility channel, high on-currents at low drain voltages are quite important. However, until 2010, the on current was lower than $1\,mA\mu m^{-1}$ even at a drain voltage of 1 V, i.e., lower than that of the Si MOSFET. This can be explained by the low carrier concentrations in the source and drain doped by ion implantation [46]. When epitaxial growth is used to form a doped source, a high carrier concentration can be obtained. Please note that the highest carrier concentration of n-GaAs is limited compared to InGaAs [47]. This feature causes difficulties in using GaAs as the n-MOS channel material. Similar problems are also reported in n-type Ge materials. A popular method for the formation of a heavily doped source is regrowth on the channel layer after patterning the gate area [48]. Partial selective etching of a heavily doped InP layer provides a similar structure [49]. For a channel length of 50 nm and drain voltage of 0.5 V, a current density of $2.4\,mA\mu m^{-1}$ was observed [49]. To my knowledge, this is the highest current density observed in FETs at a drain voltage of 0.5 V.

DOI: 10.1587/elex.13.20162002
Received July 22, 2016
Accepted August 5, 2016
Published September 25, 2016

For the formation of circuits, III–V MOSFETs must be fabricated on the Si substrate [50] because matured Si technology can then be used. For the formation on Si, two methods are generally used. One is the bonding of InGaAs thin films on Si substrates such as SOI, and the other is the direct growth on Si substrates. In the bonding scheme, when we use a compound semiconductor substrate, the diameter of the InGaAs thin film is limited to 150 mm even when MHEMT technology is used, i.e., smaller than the commercialized 300-mm Si wafer. On the other hand, direct growth on Si substrate requires a thick buffer layer (over several μm thick) to obtain good crystallinity. The thick buffer makes integration with Si circuits difficult, and increases the cost. Thus, a combination method was proposed, i.e., the InGaAs thin film splits from the Si substrate with the thick buffer, and then bonds on another Si substrate. The splitting and bonding process was confirmed using a 200-mm wafer [51]. By reusing the Si substrate with the thick buffer, the process cost can be reduced. In case of direct growth, the aspect-ratio trapping method, i.e., growth in deep trenches of SiO_2, was proposed. By trapping the defects at the sidewalls of the trenches, good crystallinity can be obtained. By eliminating the layers grown in the trenches, gate-all-around devices can be fabricated on a 300-mm wafer [52].

At present, Intel has fabricated 14-nm nodes for the Si MOS transistors. For the transition from Si to III–V, realization of the short channel is essential. To suppress the short-channel effects, Intel has introduced a fin-FET structure in the 22-nm node. As the thin channel introduces degradation in mobility [53, 54], a multi-gate structure is essential even for III–V MOSFETs. Fig. 4 shows an 8-nm-wide fin of InGaAs [55]. Digital etching reduces the fin width after mesa formation by dry etching. To realize high on-currents in the multi-gate structure, the sidewalls of the pillars must be surrounded by the heavily doped source [56] using the regrowth process.

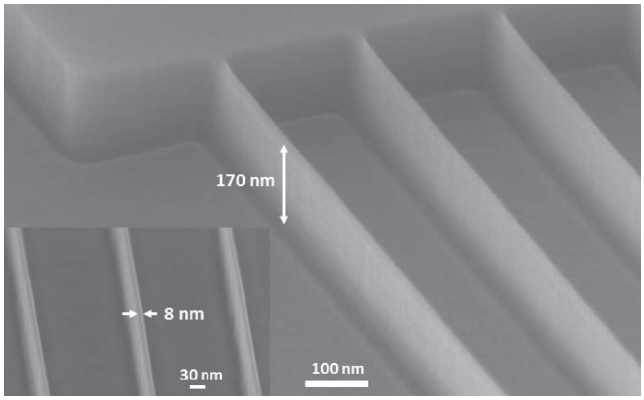

Fig. 4. SEM image of 8-nm-wide InGaAs fin. Height is 170 nm and aspect ratio is over 20 [55].

Vertical MOSFETs can realize heavily doped structures without regrowth in a multi-gate structure. Using a combination of digital etching techniques, nanowire FETs with 11-nm diameter were reported [57]. Vertical nanowires can be grown directly on the Si substrate. Moreover, introduction of heterostructures in direction

DOI: 10.1587/elex.13.20162002
Received July 22, 2016
Accepted August 5, 2016
Published September 25, 2016

of current flow can provides new device structure. For example, introduction of Type II or staggered heterojunctions can increase the on-current in tunnel FETs.

5 Conclusion

Recent progresses in the field of compound semiconductor devices were overviewed. Based on the present commercialization in consumer electronics, GaAs HEMTs were found to be essential for satellite broadcasting while GaAs HBTs play an important part in the power amplifiers of cellular phones. GaN HEMT has become popular in the power amplifiers of base stations of cellular phone systems, and the replacement of vacuum tubes is progressing. State-of-art results have also been explained, such as the 529-GHz dynamic frequency divider using InGaAs HBT, the 1-THz amplification provided by the InGaAs HEMT, and the power of 3 Wmm^{-1} at 94 GHz produced by the GaN HEMTs. The features of the InGaAs MOSFET, as the next candidate for logic circuit components, have also been explained.

Acknowledgments

A part of this work was supported by the Grant-in Aid for Scientific Research by the MEXT/JSPS and SCOPE by MIC. The author would like to thank Profs. S. Arai, M. Asada, M. Watanabe, N. Nishiyama, and S. Suzuki for their invaluable insights and expertise, which greatly assisted this research; Dr. T. Kanazawa for his technical assistance and comments; Prof. J. A. del Alamo for providing suitable figures; and finally, Mr. K. Makiyama for the critical reading of the draft.

Yasuyuki Miyamoto
received the B.S., M.S., and D.Eng. degrees in Physical Electronics from the Tokyo Institute of Technology in 1983, 1985, and 1988, respectively. He joined the Tokyo Institute of Technology after finishing the degree and is currently working as a professor of the department of electrical and electronic engineering. He was a consultant of AT&T Bell laboratories from 1994 to 1995. He is presently engaged in research on III–V semiconductor electronic devices and nanometer fabrication technology.

DOI: 10.1587/elex.13.20162002
Received July 22, 2016
Accepted August 5, 2016
Published September 25, 2016